ELSEVIER

Catalysis Today 70 (2001) 121–130

CATALYSIS TODAY

www.elsevier.com/locate/cattod

Surface morphology and reactivity of microcrystalline MgO Single and multiple acid–base pairs in low coordination revealed by FTIR spectroscopy of adsorbed CO, CD_3CN and D_2

G. Martra [a,*], T. Cacciatori [a], L. Marchese [a,b], J.S.J. Hargreaves [c], I.M. Mellor [c], R.W. Joyner [c], S. Coluccia [a]

[a] *Dipartimento di Chimica IFM, Università degli Studi di Torino, Via P. Giuria 7, I-10125 Torino, Italy*
[b] *Dipartimento di Scienze e Tecnologie Avanzate, Università del Piemonte Orientale "A. Avogadro", C.so Borsalino 54, I-15100 Alessandria, Italy*
[c] *Catalysis Research Laboratory, Nottingham Trent University, Clifton Lane, Nottingham NG11 8NS, UK*

Abstract

The surface morphology of two types of high specific surface area MgO powders (an ex-hydroxide MgO and a smoke one, eroded by H_2O and CO_2 attack) was studied by high resolution transmission electron microscopy (HRTEM) and infrared spectroscopy of adsorbed probe molecules. HRTEM images show that significant morphological defects are present on the surface of MgO microcrystals in both cases. Insights at a molecular level provided by the IR spectra of adsorbed probe molecules (CO, CD_3CN, D_2) indicate that Mg^{2+} ions on corners, edges and (1 0 0) faces are exposed in comparable amount on the surface of the microcrystals of both kind of powders. By contrast, relevant differences were found for multiple cationic sites and reactive $Mg^{2+}O^{2-}$ pairs located in region with enhanced irregularity, constituted by steep successions of steps of one unit-cell dimension. This suggests that, besides the presence of different types of single morphological defects, the presence of ensembles of such sites must be taken into account when adsorption properties and surface reactivity of different type of microcrystalline MgO materials are compared.

Keywords: MgO; Surface morphology; HRTEM; FTIR; Probe molecules

1. Introduction

MgO is often adopted as a model system in studies of dispersed oxides, because it can be easily obtained in the form of high surface area powders, and the particles, as observed by electron microscopy, are microcubes limited by (0 0 1) faces containing a series of morphological defects such as steps, terraces and kinks [1,2]. As a result, the surface is characterised by families of well-defined sites in low coordination (LC), Mg^{2+}_{LC} and O^{2-}_{LC} ions [3–5]. The coordination number is 5 (Mg^{2+}_{5C} and O^{2-}_{5C}) at the planar (0 0 1) surfaces, 4 (Mg^{2+}_{4C} and O^{2-}_{4C}) at the edges and 3 (Mg^{2+}_{3C} and O^{2-}_{3C}) at the corners of the crystals. Extensive studies have evidenced that $Mg^{2+}_{LC}O^{2-}_{LC}$ pairs in the lowest coordination are able to promote the heterolytic dissociation of X–H bonds (X = H, C, O, N, S) [6–12] or to react with CO [2,13–17], NO [18], and carbonylic compounds [19], while those on the (0 0 1) planes are essentially inert. The attention was focused on the relationship between coordination, electronic properties and reactivity of ions belonging to the different $Mg^{2+}_{LC}O^{2-}_{LC}$ pairs. These

* Corresponding author. Tel.: +39-11-670-7537/7538; fax: +39-11-670-7855.
E-mail address: martra@ch.unito.it (G. Martra).

0920-5861/01/$ – see front matter
PII: S0920-5861(01)00412-6

sites are undoubtedly responsible for the primary events of the reactivity of MgO towards adsorbed molecules, but some aspects of the overall reactivity indicated that the surrounding structure can also play a relevant role, promoting the formation of peculiar species, such as polymeric oxoanions resulting from the reaction with CO [2,17] or the reversibility or irreversibility of some reactions, such as the heterolytic dissociation of H_2 (or D_2) [6,7]. In this respect, the presence and role of multiple cationic sites, formed by ensembles of Mg^{2+} ions properly located on adjacent corners and/or edges, was postulated on the basis of the vibrational features of adsorbed species [6,7,10,17]. Two levels of surface heterogeneity can be then recognised on the surface of MgO: one is associated with the presence of ions differing for the coordination, the second resulting from the location of such ions in different surface structures. Several studies, comparing the properties of MgO powders of different origins, have shown that the relative populations of the various sites (3C, 4C, 5C) heavily depend on the morphology of the microcrystals [1,2,20], and provided preliminary information on role of surface heterogeneity [2].

In this work, further evidence about this aspect is reported on the basis of the results of an infrared investigation of various probe molecules (CO, CD_3CN, D_2) adsorbed on two types of high specific surface area MgO powders obtained through different preparation routes.

2. Experimental

Home-made ex-hydroxide MgO, hereafter referred to as MgO-h, was prepared by thermal decomposition of the parent hydroxide [2,21,22]. The $Mg(OH)_2$ powder, in the form of a self-supporting pellet, was placed in a quartz IR cell equipped with KBr windows properly designed to carry out spectroscopic measurements both at room temperature (r.t.) and liquid nitrogen temperature. The cell was connected to a conventional vacuum line (residual pressure: 1×10^{-5} Torr; 1 Torr = 133.33 Pa) allowing all thermal treatments and adsorption–desorption experiments to be carried out in situ. The hydroxide was then slowly decomposed in vacuo at ca. 523 K and finally outgassed at 1123 K. This procedure gives MgO with high specific surface area ($SSA_{BET} = 200\,m^2\,g^{-1}$) which is assumed to be completely dehydroxylated, as no OH stretching vibration bands were observed in the background IR spectrum.

The second material was a commercial MgO smoke powder, obtained by burning magnesium in air (MgO UBE 100, $SSA_{BET} = 95\,m^2\,g^{-1}$). This powder had been stored in air for months before use, exposed to the attack of water and CO_2 present in the atmosphere; it will be hereafter referred to as MgO-sa (smoke attacked). Also this material, in the form of self-supporting pellet, was thoroughly decarbonated and dehydroxylated by outgassing in the IR cell at 1123 K.

FTIR spectra were obtained using a Bruker IFS 48 spectrometer (resolution: $2\,cm^{-1}$) equipped with an MCT detector. The spectra of adsorbed molecules are reported in absorbance, after subtraction of the background spectra of the MgO samples before adsorption.

High purity CO, D_2 (Matheson) and CD_3CN (Carlo Erba) were used. CO and D_2 were employed without any additional purification except liquid nitrogen trapping, whilst CD_3CN was purified through several freeze-pump-thaw cycles.

For high resolution transmission electron microscopy (HRTEM) studies, small portions of both types of MgO powder, outgassed at 1123 K, were suspended in isopropyl alcohol and then deposited on a copper grid coated with a lacey carbon film. Electron micrographs were obtained by a Jeol 2000 EX instrument equipped with a top entry stage.

3. Results and discussion

3.1. TEM studies

TEM images showed that MgO microcrystals in the MgO-sa sample were cubelets with an average edge length of 30 nm (evaluated on the basis of a statistical measuring of ca. 300 particles) and rounded corners. At high magnification, details of the surface of these cubelets were observed, showing terraced structures (Fig. 1). Both rounded corners and terraced structures result from the erosion due to water and CO_2 attack to the MgO microcrystals during the storage in air. In fact, MgO smoke particles stored in vacuo exhibited an almost perfect cubic shape, with highly smooth

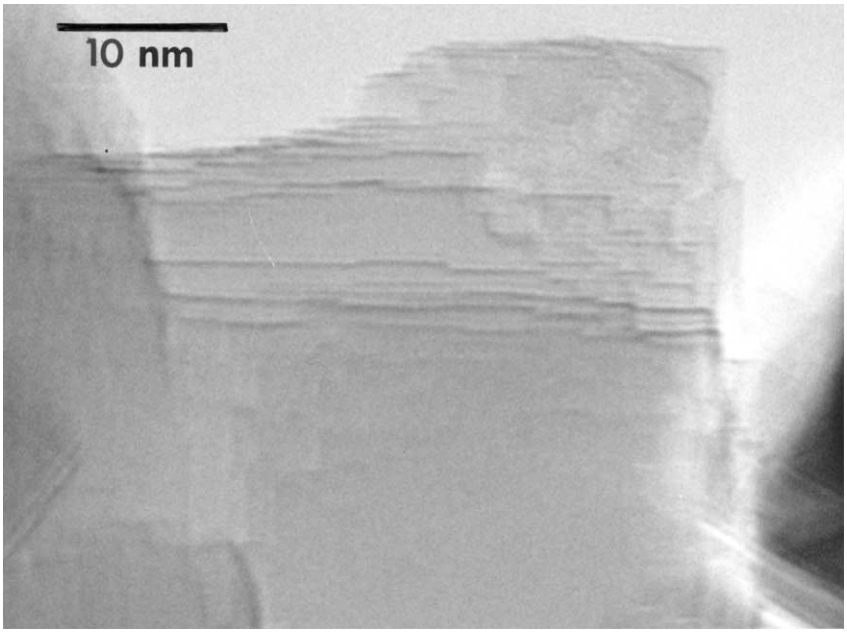

Fig. 1. Electron micrograph of the MgO-sa sample. Original magnification: ×600,000.

faces and straight borders, whereas rough surfaces and edges and rounded corners were produced by exposure to water vapour in controlled conditions [1].

In the case of MgO-h, cubic-like MgO particles were also observed, but significantly smaller in size (average edge length: 5 nm) and exhibiting steep successions of steps and terraces (Fig. 2), as reported in previous studies [2]. These morphological features well account for the measured value of SSA_{BET} (ca. $200\,m^2\,g^{-1}$).

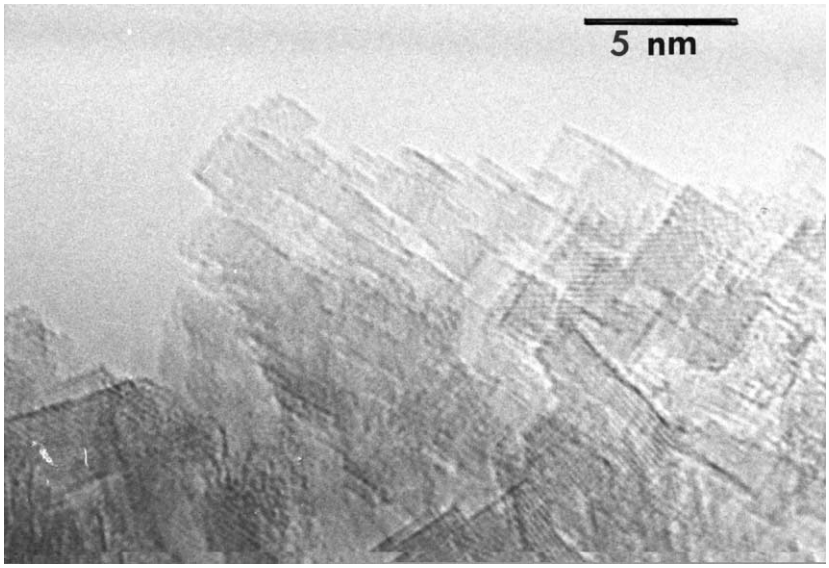

Fig. 2. Electron micrograph of the MgO-h sample. Original magnification: ×800,000.

The comparison between the HRTEM images of the two MgO powders evidences that in both cases, morphological defects are present in relevant amount on the surface of the microcrystals, although corner and edge terminations seem to be less abundant in the MgO-sa sample.

To obtain a more detailed estimation of the relative population of Mg^{2+} and O^{2-} ions in different LC in the two cases, an investigation at a molecular level of the surface of the MgO powders has been carried out by studying the vibrational features of adsorbed probe molecules.

3.2. FTIR spectra of adsorbed species

3.2.1. Preliminary remarks

The adsorption of molecules on the surface of MgO can produce: (i) reactions with $Mg^{2+}_{LC}O^{2-}_{LC}$ couples which, due to the very low concentration of both cation and anion (LC = 4C, 3C), behave as strong acid–base pairs able to promote the heterolytic dissociation of X–H bonds (X = H, C, N, O, S) or the nucleophilic attack of a highly basic O^{2-} ion to the carbon atom of CO, CO_2 or carbonylic functionalities of molecules polarised on the adjacent Mg^{2+} cations; (ii) molecular adsorption on Mg^{2+} or O^{2-} sites which belong to $Mg^{2+}O^{2-}$ pairs where one or both ions exhibit a weak Lewis acid or basic character, respectively; in this case, the adsorptive features of Mg^{2+} and O^{2-} ions can be monitored separately.

In this study, probe molecules sensitive only to reactive $Mg^{2+}O^{2-}$ pairs (i.e. D_2) or both to Lewis acid Mg^{2+} sites and acid–base $Mg^{2+}O^{2-}$ pairs (CO, CD_3CN) were used. For the sake of clarity, the data dealing with Mg^{2+} ions and reactive $Mg^{2+}_{LC}O^{2-}_{LC}$ couples will be presented and discussed in separate sections.

3.2.2. Relative abundance of single and multiple Mg^{2+} sites

3.2.2.1. CO adsorption at 77 K. The adsorption of CO on Lewis acid sites such as Mg^{2+}_{LC} produces IR bands at frequencies higher than the stretching frequency of the free molecule in the gas phase. Consequently, surface features of MgO-h related to the presence of single Mg^{2+}_{LC} cations and of multiple Mg^{2+}_{LC} sites were investigated by IR spectroscopy of

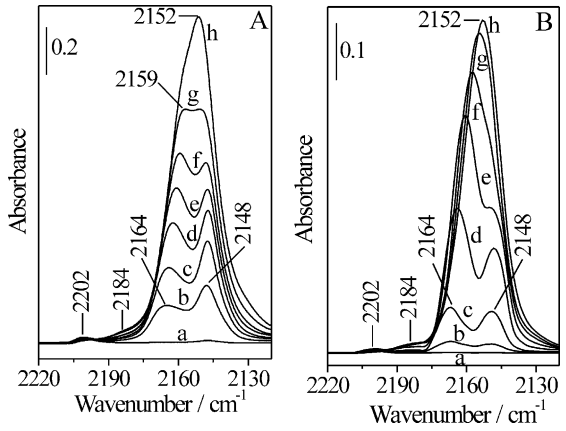

Fig. 3. IR spectra in the 2220–2120 cm^{-1} range of CO adsorbed at 77 K on MgO-h (section A) and MgO-sa (section B). Curves a–h in both sections are spectra recorded under increasing pressure of CO from: (a) 0.02 Torr to (h) 10 Torr.

CO adsorbed at 77 K [2]. A typical spectral pattern observed in the 2220–2120 cm^{-1} range at increasing CO coverage is reported in Fig. 3A. At very low CO coverage, only a weak band at 2202 cm^{-1} is present (Fig. 3A, a). By increasing the amount of adsorbed CO, this band progressively vanishes and is replaced by a new component at 2184 cm^{-1} (Fig. 3A, b–h); at the same time, a band at 2164 cm^{-1} appears, progressively shifting to 2159 cm^{-1}, while another absorption grows in at 2148 cm^{-1} (Fig. 3A, b–f). At even higher CO coverage, these two components merge in a complex band characterised by a quite flat and broad maximum, due the appearance of a new component located at ca. 2155 cm^{-1} (Fig. 3A, g). This absorption becomes the dominant spectral feature at the highest CO coverage and shifts to 2152 cm^{-1} (Fig. 3A, h).

The progressive outgassing of CO resulted in a sequence of spectra almost inverse to that observed by increasing the CO coverage: absorptions at 2152, 2159 (shifting to 2164 cm^{-1}) and 2148 cm^{-1} disappeared in the order, while the component at 2184 cm^{-1} was transformed in the weak signal at 2202 cm^{-1}, which was not reversible by outgassing at 77 K (spectra not reported).

On the basis of their position, relative intensity and reversibility, the bands at 2202, 2164–2159 and 2155–2152 cm^{-1} were assigned to CO molecules polarised on Mg^{2+}_{3C}, Mg^{2+}_{4C} and Mg^{2+}_{5C} single sites, respectively [2]. The shifts from 2164 to 2159 cm^{-1}

and from 2155 to 2152 cm^{-1} are due to dynamic and static adsorbate–adsorbate interactions among CO oscillators at high coverage. As for the 2202 cm^{-1} component, recent ab initio and DFT calculations on cluster models evidenced that its transformation in the absorption at 2184 cm^{-1} can be attributed to the addition of a second CO molecule to the CO–Mg^{2+}_{3C} adduct, resulting in the formation of a dicarbonylic species [23].

The 2148 cm^{-1} band is due to CO molecules bridged, through the carbon atom, over pairs of Mg^{2+}_{4C} and Mg^{2+}_{5C} sites at one-unit-cell steps [24].

All these components were present in the spectra of CO adsorbed at 77 K on MgO-sa (Fig. 3B), indicating that also this sample exhibits a significant amount of cationic sites in corner and edge positions. It is worth noticing that in the case of almost perfect MgO smoke cubelets, only a sharp component due to CO molecules polarised on Mg^{2+}_{5C} sites was observed, as in that case the overwhelming surface terminations of MgO crystallites are extended (0 0 1) faces with a smoothness down to the level of few angstroms [2,25].

Some differences in bandshape, dependence on the CO coverage and relative intensities are observed with respect to the case of MgO-h. For the MgO-sa sample, the band at 2164–2159 cm^{-1}, due to CO molecules adsorbed on Mg^{2+}_{4C} ions on edges, appears narrower and better resolved, so that it can be clearly observed that its shift to lower frequency as the CO coverage is increased results from the succession of formation/depletion of a series of absorptions progressively located at lower frequency (Fig. 3B, c–h). Such behaviour can be ascribed to the creation/destruction of mono-dimensional clusters of CO oscillators on the edges of MgO microcrystals, their size progressively increasing as the amount of adsorbed CO increases. It may be of interest to note that a similar behaviour was observed for two-dimensional CO clusters on regular crystal planes [25,26], whilst to our knowledge no evidence of such a phenomenon for mono-dimensional array of CO oscillators has been reported so far.

Furthermore, the downward shift of these components as the CO coverage increases seems to be larger, and finally this signal merges into the growing band due to CO molecules adsorbed on cations on (0 0 1) faces. As a result, a quite well shaped and symmetric peak centred at 2152 cm^{-1} is observed (Fig. 3B, h), without the evident shoulder observed at ca. 2159 cm^{-1} in the case of MgO-h (Fig. 3A, h). As both the bandwidth and the entity of the shift depend on the number of coupled oscillators [27–29], it appears that the coupling among CO molecules adsorbed on edges of MgO-sa involves a larger number of oscillators than in the case of MgO-h. Therefore, if cationic sites which accommodate the adsorbed species are considered, it can be concluded that MgO-sa microcrystals exhibit more regular edges, exposing longer array of Mg^{2+}_{4C} cations. More regular edges should result in a lower number of corner sites, and indeed the components at 2202 and 2184 cm^{-1}, due to mono- and dicarbonyl adduct on Mg^{2+}_{3C}, respectively, exhibit a slightly lower relative intensity with respect to the band due to CO molecules stabilised on edges and terraces. Besides the differences in the features related to CO adsorbed on the three families of single Mg^{2+}_{LC} ions, it can be noticed that the main difference in the spectral pattern of CO adsorbed on the two types of MgO deals with the band at 2148 cm^{-1}, assigned to CO molecules adsorbed on two cations at steps of a unit-cell dimension. In the case of MgO-sa, this component appears significantly reduced in intensity with respect to the other absorptions (Fig. 3B), strongly suggesting that this kind of steps is less abundant on the relatively more regular MgO-sa powder.

3.2.2.2. CD_3CN adsorption at r.t. In order to further investigate differences between the extension of the "one unit-cell roughness" of the two MgO powders, the adsorption of CD_3CN was studied. The admission of successive small doses of CD_3CN on MgO-h produced in the spectral region of the ν(CN) band two absorptions at 2317 and 2293 cm^{-1} (Fig. 4A), which were assigned to CD_3CN molecules bridged by the nitrogen atom on two Mg^{2+}_{4C} sites on adjacent steps and to molecules linearly adsorbed on single Mg^{2+}_{4C} sites, respectively [30]. The same experiment was performed with MgO-sa, and in this case the component at 2317 cm^{-1} appeared strongly reduced in intensity with respect to the main band at 2293 cm^{-1} (Fig. 4B), confirming that steps of one unit-cell dimension are less abundant on this type of MgO powder.

On the basis of the spectroscopic features of adsorbed CO and CD_3CN commented on above, it can be concluded that the MgO-h and MgO-sa samples appear quite different if the relative amount of one unit-cell dimension steps is considered. Apparently,

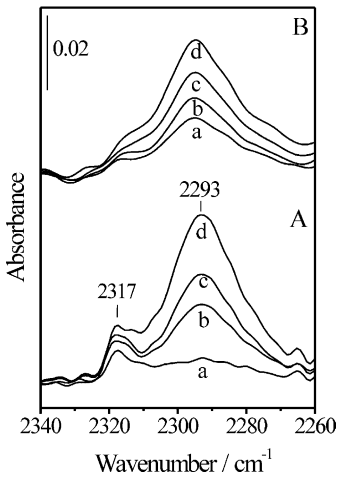

Fig. 4. IR spectra in the 2340–2260 cm^{-1} range of CD_3CN adsorbed at r.t. on MgO-h (section A) and MgO-sa (section B). Curves a–d in both sections are spectra recorded under increasing pressure of CD_3CN: (a) 0.02; (b) 0.05; (c) 0.08; (d) 0.15 Torr.

this kind of surface structure is less abundant on the MgO smoke sample exposed to the attack of water and CO_2 during its storage in air. Similarities and differences in the types of single and multiple Mg^{2+}_{LC} sites exposed at the surface of the two MgO powders, as monitored by the IR bands of adsorbed CO and CD_3CN, are summarised in Table 1.

To investigate if such differences in surface morphology resulted in some difference in the reactivity of the two kinds of MgO powders as well, the formation of anionic species by contact with CO both at 77 K and at r.t. and the heterolytic dissociation of D_2 at r.t. were studied.

3.2.3. Influence of the surface roughness on the reactivity of MgO

3.2.3.1. Reactivity towards CO at 77 K. Extensive studies evidenced that, besides the polarisation on cationic sites, the adsorption of carbon monoxide on thoroughly dehydroxylated MgO results in the formation of anionic species, which are produced by nucleophilic attack of basic O^{2-}_{LC} sites exposed in the lowest coordination (3C) onto the surface of MgO microcrystals to CO molecules stabilised on adjacent Mg^{2+}_{LC} cations [2,13–17]. At low temperature, such reactivity is limited to the production of monomeric CO_2^{2-}, dimeric $C_2O_3^{2-}$ and trimeric $C_3O_4^{2-}$ species [16,17]. The IR spectral features of dimers and trimers observed after admission at 77 K of 10 Torr CO on MgO-h are shown in Fig. 5a. Following the established band assignment and labelling [17], the peak at 1473 cm^{-1} (T′) can be ascribed to dimeric species, while the other signals result from the overlapping of the absorption due to two families of trimeric anionic adducts, KD_1 and KD_2. It can be noticed that in the complex absorptions at 2100–2000, 1600–1500 and 1400–1300 cm^{-1}, where the contributions due to the two species are partially resolved, the components assigned to KD_1 species appear significantly more intense than those ascribed to the KD_2 ones. No signal related to monomeric CO_2^{2-} species was detected, as at this level of CO coverage they are fully transformed into the dimeric ones.

Similar features were observed in a parallel experiment carried out on MgO-sa. In this case, besides the lower intensity of the overall spectral pattern, reflecting the lower specific surface area of this sample, the signals due to trimeric species are dominated by the

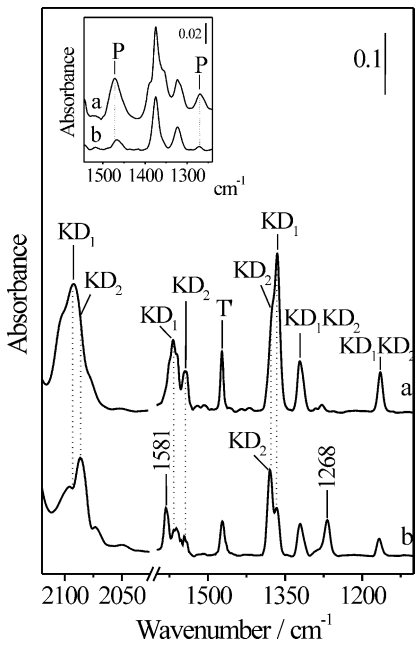

Fig. 5. IR spectra in the 2120–1000 cm^{-1} range of CO (10 Torr) adsorbed at 77 K on: (a) MgO-h and (b) MgO-sa. In the inset are the spectra obtained after contact with 10 Torr CO at r.t. for 10 h: (a) MgO-h and (b) MgO-sa.

Table 1
Types of Mg^{2+} ions in low coordination exposed on the surface of MgO-h and Mg-sa powders outgassed at 1123 K as revealed by the IR bands of adsorbed CO (at 77 K) and CD_3CN (at r.t.)[a]

Sample	Cationic site					
	Mg^{2+}_{3C}	Mg^{2+}_{4C}		Mg^{2+}_{5C}	Mg^{2+}_{4C}–Mg^{2+}_{5C} pairs at a one unit-cell step	Mg^{2+}_{4C}–Mg^{2+}_{4C} pairs on adjacent unit-cell steps
Bands (position in cm^{-1}) due to adsorbed:						
CO (ν_{CO})	ν_{CO}: 2202[b]	ν_{CO}: 2159[c]		ν_{CO}: 2152[c]	ν_{CO}: 2148[b]	
CD_3CN (ν_{CN})			ν_{CN}: 2293			ν_{CN}: 2317
MgO-h	+	+	+	+	+	+
MgO-sa	−	+	+	+	−	−

[a] Signs (+) and (−) indicate high and low relative intensity of spectral components, respectively.
[b] At low CO coverage.
[c] At high CO coverage.

KD_2 components (Fig. 5b). Furthermore, two new bands are observed at 1581 and 1268 cm^{-1}.

As KD_1 and KD_2 species have very similar spectra, and, consequently, similar geometric and electronic structures, the small differences must be ascribed to differences in surrounding surface structures. It has been shown in the previous section that MgO-h exhibits steps of the order of unit-cell dimensions into a larger extent with respect to MgO-sa. It can be proposed that the formation of KD_1 species mainly occurs in the parts of the MgO microcrystals where this kind of surface roughness is present, and, specifically, by reaction of CO with O^{2-}_{3C} ions located in corner position where the edges of such steps intersect.

This proposal is in agreement with previous observations that only KD_1 species can evolve into larger polymeric anions adducts resulting from the merging of KD_1 trimers formed on defect sites on adjacent steps [17]. Confirmatory evidences of this statement were obtained by CO adsorption at r.t. In these conditions, in the case of MgO-h intense bands due to polymeric species (labelled as P in the inset of Fig. 5) grew at the expenses of the KD_1 components, whereas for the MgO-sa sample, where the trimeric species are mainly of the KD_2 type, only traces of components due to polymers were observed (inset Fig. 5, curves a and b, respectively).

Finally, the bands at 1581 and 1268 cm^{-1} observed in the spectrum of CO adsorbed on MgO-sa must be commented on. Systematic experiments evidenced that they are related to the same species and are immediately destroyed upon oxygen admission. On the basis of these observations, it can be inferred that these components are due to two vibrational modes of a reduced species. Carbon monoxide can be easily reduced at the surface of MgO, i.e. by interaction with surface F-type centres [31,32]. These defects cannot be formed on the surface of pure MgO crystallites by simply outgassing at high temperature, while they can be produced in the presence of metal impurities. It can be then supposed that few of these sites are present in the MgO-s a sample, perhaps due to the presence of traces of metallic magnesium left unburned during the preparation of this kind of MgO powder. Additional IR, EPR and UV–Vis experiments devoted to a deeper investigation of this point and to the recognition of the nature and structure of the reduced species are in progress.

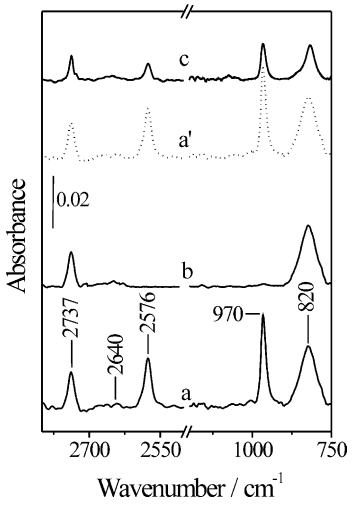

Fig. 6. IR spectra of D_2 adsorbed at r.t. on: (a) MgO-h, in the presence of 200 Torr D_2; (b) MgO-h, after subsequent outgassing 10 min at r.t.; (c) MgO-sa, in the presence of 200 Torr D_2. Curve a′ as curve a reported for the sake of comparison.

3.2.3.2. Heterolytic dissociation of D_2 at r.t. Further insights on the influence of the surrounding structure on the reactivity of $Mg^{2+}_{LC}O^{2-}_{LC}$ were obtained by studying the adsorption of D_2. The IR spectrum of D_2 (200 Torr) adsorbed on MgO-h is shown in Fig. 6. Two sets of bands are present, one exhibiting three absorptions at 2737, 2640 (very weak and broad) and 2576 cm^{-1}, and the second comprising two peaks at 970 (narrow) and 820 (broader) cm^{-1} (Fig. 6a). The 2576 and 970 cm^{-1} components disappeared after evacuation of the D_2 at r.t., whereas the weak signal at 2640 cm^{-1} and the bands at 2737 and 820 cm^{-1} were left essentially unchanged (Fig. 6b). A subsequent D_2 readimission restored the initial spectral pattern (not reported). The bands observed in the 2800–2500 and 1000–800 cm^{-1} ranges were attributed to the stretching vibrations of deuteroxyl (OD) and deuteride (MgD) species, respectively, derived from the heterolytic dissociation of deuterium molecules on $Mg^{2+}_{LC}O^{2-}_{LC}$ pairs in the lowest coordination [6,7]. The peak at 2737 cm^{-1} is most likely due to isolated three-coordinated OD species. The 2576 cm^{-1} component can be assigned to the stretching mode of OD groups with a similar coordination; its lower frequency is likely due to H-bond interactions with suitably located neighbouring surface oxygen anions on adjacent corner position [7]. On the other hand, the bandwidth

of this signal ($\sim$20 cm^{-1}) is unusually small when compared with conventional H-bond formation in the gas phase or in liquids [33] as well as on solid surfaces [34,35]. It can be proposed that in the present case, the proton donor and the proton acceptor form a relatively rigid framework, which does not favour an efficient coupling of intra- and intermolecular modes as observed in H-bonded molecular aggregates [36].

The weak and broader signal centred at 2640 cm^{-1} could be attributed to another minor fraction of hydrogen bonded OD groups. The surrounding structure of this species might differ to some extent from the 2576 cm^{-1} OD groups, resulting in a different hydrogen bonding and therefore a different shift of the OD band. Furthermore, the broader bandwidth indicates that in this case, proton donor and proton acceptors form a less rigid framework.

The second set of bands at 970 and 820 cm^{-1} have been attributed to linear (MgD) and bridged (Mg_nD) deuteride species, respectively. In the latter case, on the basis of strong analogies with the IR features of MgH_2 [6,7] the bridged D^- anions should be stabilised by three Mg^{2+}_{3C} cations suitably located in three adjacent corner positions, simulating a (1 1 1) microplane. It is clear from these results that two different processes of D_2 heterolytic dissociations occur. The deuteroxyl groups absorbing at 2737, and deuteride species responsible for the band at 820 cm^{-1} are essentially unaffected by D_2 desorption at r.t. and are produced through an irreversible splitting of D_2 molecules, whereas the OD and MgD species characterised by the 2576 and 970 cm^{-1} peaks, respectively, that disappear after D_2 evacuation, must be formed through a reversible D_2 dissociation.

The same experiment was performed with the MgO-sa sample, and both sets of bands due to the irreversible and reversible splitting of D_2 molecules were observed (Fig. 6c). Because of the lower specific surface area, the overall spectral pattern appeared less intense, and with some significant changes in the relative intensity of the various components. In fact, the 2576 and 970 cm^{-1} peaks due to reversible deuteroxyl and deuteride species appeared reduced in intensity with respect to the components due to irreversible OD and MgD.

As stated above, the position of the band attributed to the reversible deuteroxyls suggested that this species interacts through hydrogen bonding with anions located on nearby corners. Apparently, structures of this kind, resulting from the presence of O^{2-}_{3C} in corner positions on adjacent steps of a unit-cell dimension, are less abundant on the surface of MgO-sa microcrystals.

4. Conclusions

The study by IR spectroscopy of the adsorption of CO, CD_3CN and D_2 allowed the evaluation of the relative amount of single and multiple surface sites on two types of MgO powders.

The results obtained by CO and CD_3CN adsorption indicated that the relative population of single Mg^{2+} ions with different coordination (3C, 4C, 5C) is similar for the two samples investigated, while the occurrence of double cationic sites constituted by two cations at steps of a unit-cell dimension is significantly different in the two cases. The microcrystals of both MgO powders exhibited $Mg^{2+}O^{2-}$ couples able to react with CO and D_2. However, in the case of the sample with higher specific surface area, this reactivity appeared more markedly affected by the structure surrounding these reactive pairs, suggesting that they are located in regions with enhanced irregularity, resulting perhaps from a surface roughness at a one unit-cell dimension.

The overall collection of spectroscopic data suggest that not only the relative amount of surface sites in LC (Mg^{2+} or $Mg^{2+}O^{2-}$ pairs), but also their location in different surrounding structures must be considered in the investigation of the surface adsorptive and reaction behaviour of MgO. This can become even more important in the evaluation of the structure sensitivity character of specific reactions.

Acknowledgements

Ube Industries is acknowledged for the kind provision of the 100A material. Italian and UK authors are grateful to Ministero per la Ricerca Scientifica e Tecnologica (MURST) and EPSRC, respectively, for financial support.

References

[1] S. Coluccia, A.J. Tench, R.L. Segall, J. Chem. Soc., Faraday Trans. I 75 (1979) 1769 and references therein.

[2] S. Coluccia, M. Baricco, L. Marchese, G. Martra, A. Zecchina, Spectrochim. Acta A 49 (1993) 1289.
[3] S. Coluccia, M. Deane, A.J. Thench, J. Chem. Soc., Faraday Trans. I 74 (1978) 2913.
[4] E. Giamello, E. Garrone, P. Ugliengo, J. Chem. Soc., Faraday Trans. I 85 (1989) 1373.
[5] E.V. Stefanovich, T.N. Truong, J. Chem. Phys. 102 (1995) 5071.
[6] S. Coluccia, F. Boccuzzi, G. Ghiotti, C. Mirra, Z. Phys. Chem. NF 121 (1980) 141.
[7] E. Knözinger, K.-H. Jacob, P. Hofmann, J. Chem. Soc., Faraday Trans. 89 (1993) 1101.
[8] M. Che, S. Coluccia, A. Zecchina, J. Chem. Soc., Faraday Trans. I 74 (1978) 1324.
[9] V.A. Shvets, A.V. Kuznetov, V.A. Fenin, V.B. Kazansky, J. Chem. Soc., Faraday Trans. I 81 (1985) 2913.
[10] M. Bensitel, O. Saur, J.C. Lavalley, Mater. Chem. Phys. 28 (1991) 309.
[11] G. Martra, E. Borello, E. Giamello S. Coluccia, in: H. Hattori, M. Misono, Y. Ono (Eds.), Proceedings of the International Symposium on Acid–Base Catalysis II, Kodansha/Elsevier, Tokyo/Amsterdam, 1994, p. 169 and references therein.
[12] E. Knözinger, K.-H. Jacob, S. Singh, P. Hofmann, Surf. Sci. 290 (1993) 388.
[13] A. Zecchina, F.S. Stone, J. Chem. Soc., Chem. Commun. (1974) 582.
[14] E. Guglielminotti, S. Coluccia, E. Garrone, L. Cerruti, A. Zecchina, J. Chem. Soc., Faraday Trans. I 75 (1979) 96.
[15] R.M. Morris, K.J. Klabunde, J. Am. Chem. Soc. 105 (1983) 2633.
[16] M.A. Babaeva, D.S. Bystrov, A.Yu. Kovalgin, A.A. Tsyganenko, J. Catal. 123 (1990) 396.
[17] A. Zecchina, S. Coluccia, G. Spoto, D. Scarano, L. Marchese, J. Chem. Soc., Faraday Trans. 86 (1990) 703 and reference therein.
[18] L. Cerruti, E. Modone, E. Guglielminotti, E. Borello, J. Chem. Soc., Faraday Trans. I 70 (1974) 729.
[19] E. Garrone, D. Bartalini, S. Coluccia, G. Martra, D. Tichit, F. Figueras, in: H. Hattori, M. Misono, Y. Ono (Eds.), Proceedings of the International Symposium on Acid–Base Catalysis II, Kodansha/ Elsevier, Tokyo/Amsterdam, 1994, p. 183 and references therein.
[20] A.F. Moodie, C.E. Warble, J. Cryst. Growth 10 (1971) 26.
[21] R.L. Nelson, J.W. Hale, Discuss. Faraday Soc. 52 (1971) 77.
[22] E. Garrone, A. Zecchina, F.S. Stone, Phil. Mag. B 42 (1980) 683.
[23] A.G. Pelmenshikov, G. Morosi, A. Gamba, S. Coluccia, G. Martra, L.G.M. Petterson, J. Phys. Chem. 104 (2000) 11497.
[24] R. Soave, G. Pacchioni, Chem. Phys. Lett. 320 (2000) 345.
[25] L. Marchese, S. Coluccia, G. Martra, A. Zecchina, Surf. Sci. 269/270 (1992) 135.
[26] A. Zecchina, D. Scarano, S. Bordiga, G. Ricchiardi, G. Spoto, F. Geobaldo, Catal. Today 27 (1996) 403 and references therein.
[27] P. Hollins, J. Pritchard, Surf. Sci. 89 (1979) 486.
[28] P. Hollins, J. Pritchard, in: R.F. Willis (Ed.), Vibrational Spectroscopy of Adsorbates, Springer, Berlin, 1980, p. 125.
[29] R. Disselkamp, H. Chang, G.E. Ewing, Surf. Sci. 240 (1990) 193.
[30] A.G. Pelemenschikov, G. Morosi, A. Gamba, S. Coluccia, G. Martra, E.A. Paukshtis, J. Phys. Chem. 100 (1996) 5011.
[31] L. Marchese, S. Coluccia, G. Martra, E. Giamello, A. Zecchina, Mater. Chem. Phys. 29 (1991) 437.
[32] E. Giamello, D. Murphy, L. Marchese, G. Martra, A. Zecchina, J. Chem. Soc., Faraday Trans. 89 (1993) 3715.
[33] G.C. Pimentel, A.L. McClellan, The Hydrogen Bond, Freeman, San Francisco, 1960.
[34] H.P. Boehm, H. Knözinger, in: J.R. Anderson, M. Boudart (Eds.), Catalysis: Science and Technology, Springer, Berlin, Vol. 4, 1983, p. 39.
[35] A. Novak, Struct. Bonding (Berlin) 18 (1974) 177.
[36] A.M. Ferrari, G. Pacchioni, J. Phys. Chem. 99 (1995) 17010.